

# Spectral properties of $\text{Eu}^{3+}$ -activated yttrium oxysulfide red phosphor

Yun-Hwa Tseng<sup>a</sup>, Bi-Shiou Chiou<sup>b,\*</sup>, Chao-Chi Peng<sup>c</sup>, Lyuji Ozawa<sup>c</sup>

<sup>a</sup>*Institute of Electro-Optical Engineering, Hsinchu, Taiwan*

<sup>b</sup>*Department of Electronics Engineering and Institute of Electronics, National Chiao Tung University, Hsinchu, Taiwan*

<sup>c</sup>*Electronics Research and Service Organization, Industrial Technology Research Institute, Hsinchu, Taiwan*

Received 18 September 1997; accepted 27 February 1998

## Abstract

The effects of Eu on the spectral properties of  $\text{Y}_2\text{O}_2\text{S}$  have been investigated. The  $\text{Y}_2\text{O}_2\text{S}:\text{Eu}$  phosphor powders were prepared with a flux fusion method and electrophoretically deposited on an ITO-coated glass substrate to form a thin layer. Both cathodoluminescence and photoluminescence emission spectra of  $\text{Y}_2\text{O}_2\text{S}:\text{Eu}$  were measured. The highly intense emission lines at 616 and 626 nm are attributed to the transition from  $^5\text{D}_0$  to  $^7\text{F}_2$  levels. The color of  $\text{Y}_2\text{O}_2\text{S}:\text{Eu}$  phosphor varies from orange to red as the Eu concentration increases from  $\text{Eu}/\text{Y} = 0.025$  (molar ratio) to 0.06. The luminescence decay times are shorter than 1.1 ms for Eu concentrations ranging from 0.025 to 0.06 (Eu/Y molar ratio). The luminescent color becomes redder but less bright as the Eu concentration is increased. © 1998 Elsevier Science S.A. All rights reserved.

**Keywords:** Phosphor;  $\text{Y}_2\text{O}_2\text{S}:\text{Eu}$ ; Luminescence

## 1. Introduction

Phosphors are materials that emit photons with a high luminescence efficiency. They are widely used as radiation detectors and in visual displays such as computer monitors and television screens. A display screen is a thin layer of phosphor deposited on a glass substrate by different coating methods. The luminescent materials consist of highly purified inorganic compounds doped with activator element.

$\text{Y}_2\text{O}_2\text{S}:\text{Eu}$  red phosphor, with its sharp emission line for good calorimetric definition and high luminescence efficiency, is extensively used in the phosphor screen of display devices [1,2]. However, the fabrication of good  $\text{Y}_2\text{O}_2\text{S}:\text{Eu}$  phosphor is difficult. The phosphor research is empirical in nature, despite the knowledge in solid-state physics and material science. Among the synthesis methods, the sulfuration of a mixture of yttrium and europium oxides in the flux is the most promising because it is mass producible. The flux materials usually include  $\text{Na}_2\text{CO}_3$ ,  $\text{K}_2\text{CO}_3$ ,  $\text{K}_3\text{PO}_4$ , etc. [3–5].

In this research,  $\text{Y}_2\text{O}_2\text{S}:\text{Eu}$  phosphor was fabricated with a flux fusion method previously developed by one of the authors [3]. An electrophoretic deposition method is employed to deposit a thin layer of  $\text{Y}_2\text{O}_2\text{S}:\text{Eu}$  phosphor onto an indium-tin-oxide (ITO)-coated glass. The influence

of Eu concentration on the luminescent characteristics of the yttrium oxysulfide phosphor is explored.

## 2. Experimental procedures

Europium-doped yttrium oxysulfide ( $\text{Y}_2\text{O}_2\text{S}:\text{Eu}$ ) red phosphor powders were prepared by sintering the blended mixtures of  $\text{Y}_2\text{O}_3$  (99.999),  $\text{Eu}_2\text{O}_3$  (99.99), S,  $\text{Na}_2\text{CO}_3$ ,  $\text{Li}_3\text{PO}_4$  and  $\text{K}_2\text{CO}_3$  at  $1150^\circ\text{C}$  for 2.5 h. The weight ratio of  $\text{Y}_2\text{O}_3/\text{S}/\text{Na}_2\text{CO}_3/\text{Li}_3\text{PO}_4/\text{K}_2\text{CO}_3$  is 46.7:23.4:16.4:9.4:2.3. The Eu/Y molar ratio varies from 0.025 to 0.06. After sintering, samples were washed with water to remove the residual flux and flux byproducts and then etched with 5%  $\text{HNO}_3$  solution for a clean, smooth particle surface. Details of the fabrication process is described elsewhere [3,6].

Phosphor powders were coated onto the ITO glass substrate by an electrophoretic deposition method. Electrophoretic deposition is a materials processing technique in which particles suspended in liquid are deposited on to a substrate under the influence of an applied electric field. This method is currently used in applying a thin layer of luminescent materials in the manufacturing of cathode ray tube (CRT) screens. However, the mechanisms for the transport and adhesion of the particles to the substrates are not well understood. In this study, the deposition of  $\text{Y}_2\text{O}_2\text{S}:\text{Eu}$  powders was carried out in an isopropyl alcohol (IPA) bath

\* Corresponding author.

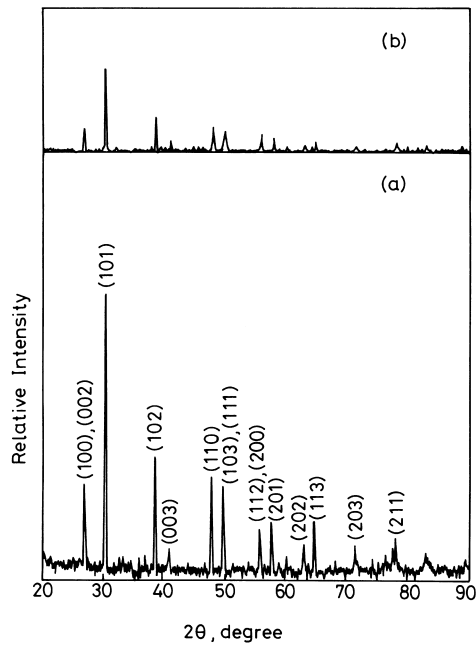


Fig. 1. X-ray diffraction patterns of  $Y_2O_2S:Eu$  with various Eu concentrations (a)  $Eu/Y = 0.025$  and (b)  $Eu/Y = 0.06$  (molar ratio).

containing magnesium nitride [6,7]. The film weight was  $2 \text{ mg/cm}^2$ .

The cathodoluminescence (CL) spectra were measured with an electron gun in a vacuum chamber. The chamber

was pumped down to  $5 \times 10^{-2}$  Torr with a mechanical pump and to  $5 \times 10^{-7}$  Torr with a turbo pump. Samples were excited by electron beam with an accelerating voltage of 10 kV and electron beam current of  $40 \mu\text{A}$ . The cathodoluminescent emission light passed through a lens to focus on an optical fiber. The light which progressed along the optical fiber was converted to an electrical signal by Fourier transform analysis instruments. The cathodoluminescence intensity was measured with a CL-SEM system (ABT-150s, Japan) with a voltage from 5 to 20 kV. The wavelength detection range was 500–700 nm.

The CIE color coordinates of phosphor were measured with a colorimeter (Minolta CS-100, Japan). The excitation source used in the CIE measurement was the electron gun employed in the CL measurement.

In the photoluminescence (PL) measurement, a pulsed Nd:YAG laser (spectra physics DCR-2) was used as the excitation source. The wavelength of the exciting source was converted to 337.1 nm before exciting the sample [6]. The photoluminescence was detected with a photon multiplier tube through a monochromator. The electrical signal was received by a photon counter through an amplifier. The photoluminescence spectra were analyzed by Asyst-4 software with a personal computer through the IEEE GPIB card. The wavelength detection range was 450–700 nm. An oscilloscope was connected to the PL measurement system to observe the decay of the photoluminescent intensity.

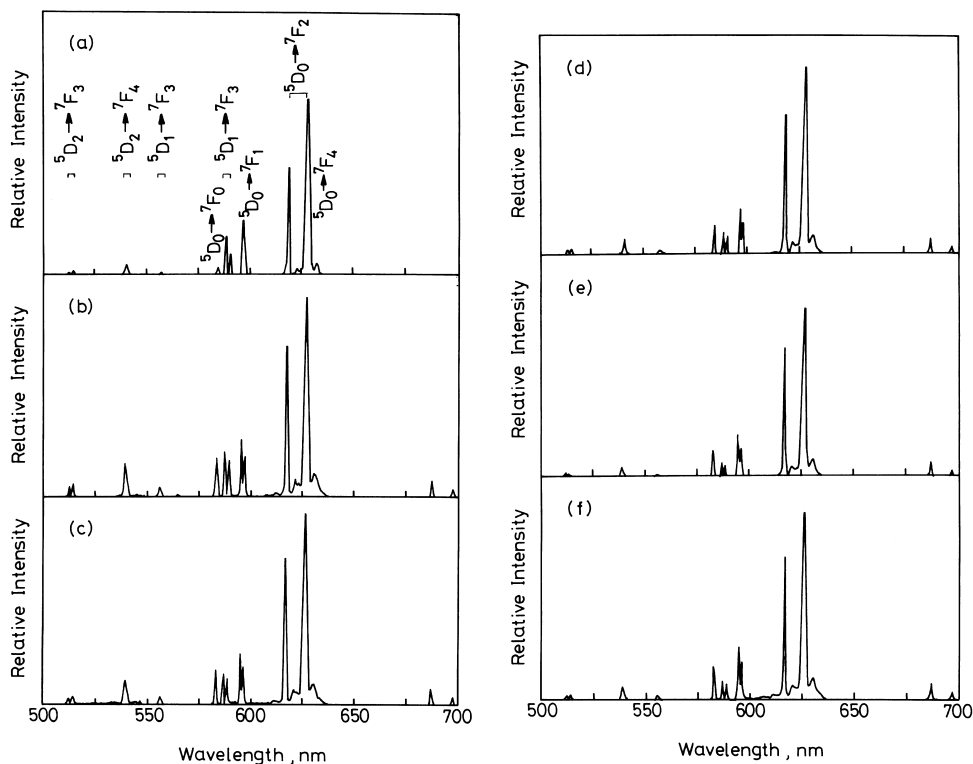


Fig. 2. The 10 kV CL spectra of  $Y_2O_2S:Eu$  phosphor with various Eu concentrations (a)  $Eu/Y = 0.025$ , (b)  $Eu/Y = 0.035$ , (c)  $Eu/Y = 0.04$ , (d)  $Eu/Y = 0.05$ , (e)  $Eu/Y = 0.055$  and (f)  $Eu/Y = 0.06$  (molar ratio).

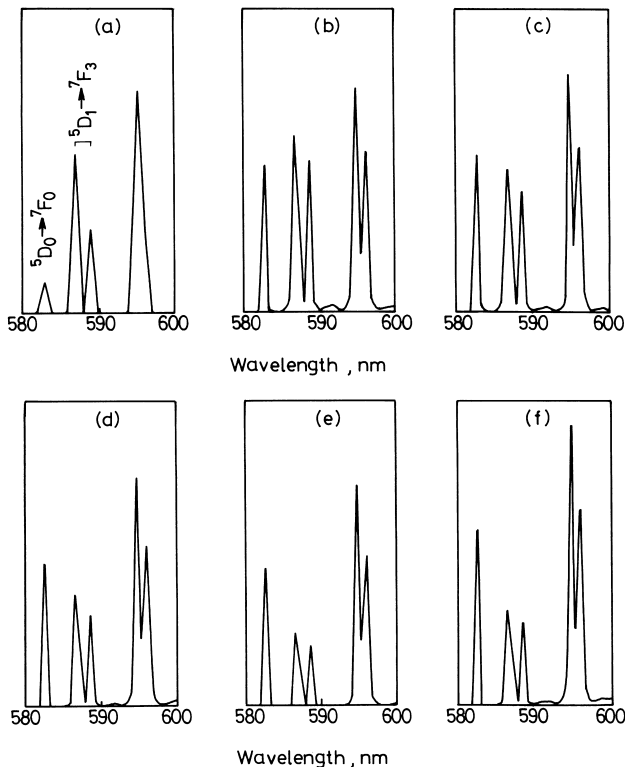


Fig. 3. The 10 kV CL spectra of  $\text{Y}_2\text{O}_2\text{S}:\text{Eu}$  phosphors between 580 and 600 nm. (a)  $\text{Eu}/\text{Y} = 0.025$ , (b)  $\text{Eu}/\text{Y} = 0.035$ , (c)  $\text{Eu}/\text{Y} = 0.04$ , (d)  $\text{Eu}/\text{Y} = 0.05$ , (e)  $\text{Eu}/\text{Y} = 0.055$  and (f)  $\text{Eu}/\text{Y} = 0.06$  (molar ratio).

### 3. Results and discussion

The X-ray diffraction analysis, shown in Fig. 1, reveals that  $\text{Y}_2\text{O}_2\text{S}:\text{Eu}$  has a hexagonal structure with unit cell dimensions  $a = 0.37$  nm and  $c = 0.65$  nm. Yttrium oxysulfide crystallizes in the  $D_{3d}^3$  ( $P\bar{3}m$ ) space group, the point

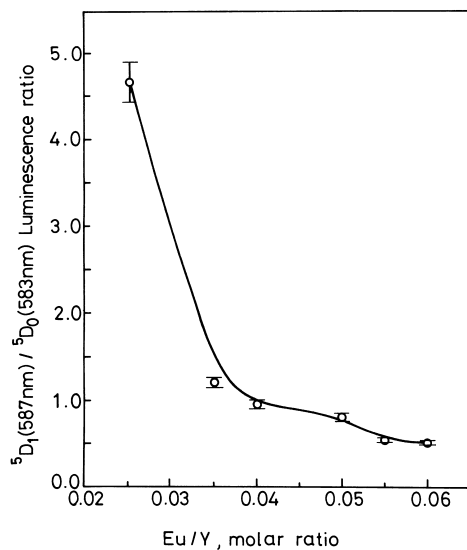


Fig. 4.  ${}^5\text{D}_1(587\text{ nm})/{}^5\text{D}_0(583\text{ nm})$  luminescence ratio as a function of  $\text{Eu}/\text{Y}$  ratio for  $\text{Y}_2\text{O}_2\text{S}:\text{Eu}$  phosphor.

symmetry of the yttrium site being  $C_{3v}$  ( $3m$ ) [8]. The europium ion was expected to occupy the yttrium site in  $\text{Y}_2\text{O}_2\text{S}:\text{Eu}$ , since the ionic radius of  $\text{Eu}^{3+}$  (0.95 Å) is slightly larger than that of  $\text{Y}^{3+}$  (0.89 Å) [9]. The electron transition of  $\text{Y}_2\text{O}_2\text{S}:\text{Eu}$  occurs from the  ${}^5\text{D}_J$  ( $J = 0, 1, 2, 3$ ) levels to  ${}^7\text{F}_J$  ( $J = 0$  to 6) levels. Some emission lines are eliminated by the selection rule and some are too weak to be observed [10]. Fig. 2 exhibits the cathodoluminescent emission spectra between 500 and 700 nm for samples with various Eu concentration. The strongest red-emission lines at 626 and 616 nm as shown in Fig. 2 are due to transition from  ${}^5\text{D}_0$  to  ${}^7\text{F}_2$  level. The most important line at 626 nm is the strongest emission light for the red color. In the orange-emission lines, the wavelengths of 587 and 590 nm emission light are apparent at room temperature. They are produced by the electron transition from  ${}^5\text{D}_1$  to  ${}^7\text{F}_3$  (587 nm) and  ${}^5\text{D}_0$  to  ${}^7\text{F}_1$  (590 nm) levels. Another emission at the green-emitting region is the 538 nm emission light for the electron transition from the  ${}^5\text{D}_2$  to  ${}^7\text{F}_4$  level. At wavelengths larger than 626 nm, only two small peaks are observed for the electron transition from  ${}^5\text{D}_0$  to  ${}^7\text{F}_4$ . The spectra of samples with various Eu concentration is similar, suggesting that the main electron level is from  ${}^5\text{D}_0$  to  ${}^7\text{F}_2$  to provide the red-emitting light.

Fig. 3 exhibits three luminescence lines between wavelengths 583 and 587 nm which correspond to the transitions  ${}^5\text{D}_0$  to  ${}^7\text{F}_0$ , and  ${}^5\text{D}_1$  to  ${}^7\text{F}_3$ , respectively. When Eu concentration varies, the peak intensity varies. The 583 nm peak becomes stronger than the 587 nm peak when Eu concentration increases from 2.5 to larger than 4. It means the electron transitions from  ${}^5\text{D}_0$  becomes important. The  ${}^5\text{D}_1$  to  ${}^5\text{D}_0$  luminescence intensity ratio was calculated and plotted as a function of Eu concentrations as shown in Fig. 4. The intensity ratio decreases as Eu concentration increases.

A similar trend was reported by Ozawa that the  ${}^5\text{D}_1/{}^5\text{D}_0$  intensity ratio decreased with the increase of Eu concentration. Since  ${}^5\text{D}_0$  cathodoluminescence contributes mainly to improving the brightness, the brightness decreases as Eu concentration is increased [11].

In the PL measurement, the 337.1 nm light excites  $\text{Eu}^{3+}$  ions from ground state to the charge transfer state at 365 nm. Fig. 5 exhibits the PL spectra for samples with various Eu contents. The ground state of Eu electron configuration is  ${}^7\text{F}_0$  and the electron outer shell configuration is inclusive of  $4f^n$ ,  $4f^{n-1}5d$ ,  $4f^{n-1}6p$  levels. The electron transition of  $\text{Eu}^{3+}$  must obey the selection rule ( $\Delta J(1, 0$  and  $\Delta l(1)$ ). The  $\text{Eu}^{3+}$  crystal spectra classify into  ${}^7\text{F}$  multiple and lower levels of  ${}^5\text{D}$  multiple.

Photoluminescence is different from cathodoluminescence in the excitation source. Photoluminescent emission depends strongly on the excitation energy  $h\nu$ , which can be used for selective excitation of a particular emission process. One of the fundamental differences between PL and CL is that a photon only generates one electron-hole pair, but an electron can generate thousands of electron-hole

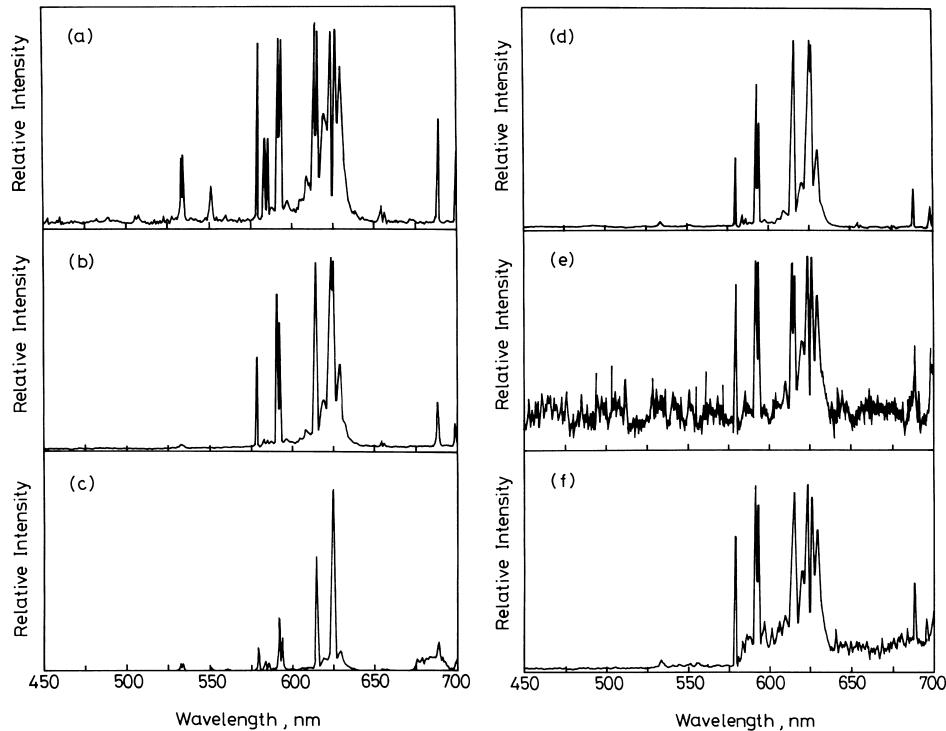


Fig. 5. PL spectra of  $Y_2O_2S:Eu$  phosphor with various Eu concentration, (a)  $Eu/Y = 0.025$ , (b)  $Eu/Y = 0.035$ , (c)  $Eu/Y = 0.04$ , (d)  $Eu/Y = 0.05$ , (e)  $Eu/Y = 0.055$  and (f)  $Eu/Y = 0.06$  (molar ratio).

pairs in the excitation volume. The difference between PL and CL is also in penetration depth. The CL causes the excess carriers that will be affected by a possible gradient in the concentration of electrically active impurities and defects that can cause electric field-induced carrier drift in addition to carrier diffusion.

The spectra lines of PL at 616 and 626 nm ( $^5D_0 \rightarrow ^7F_2$ ) is similar to what CL measured, as shown in Figs. 2 and 5. The emission peaks at  $\sim 530$  nm ( $^5D_1 \rightarrow ^7F_2$ ) and  $\sim 583$  nm ( $^5D_0 \rightarrow ^7F_0$ ) for samples with  $Eu/Y(0.025)$  are weaker than those of sample  $Eu/Y = 0.025$ , as seen in Fig. 5. This may be due to the so-called true activator saturation effect [12–14].

Saturation of light output with increasing pumping density is primarily a kinetic problem. The most probable

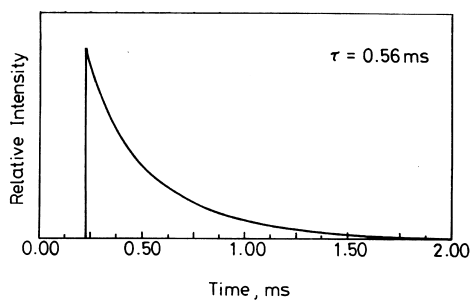


Fig. 6. Relative intensity of 626 nm emission line as a function of time for  $Y_2O_2S:Eu$  phosphor.  $Eu/Y = 0.06$  (molar ratio). The decay time  $\tau$  is the time the intensity reduced to  $1/e$  of the original value.

causes of saturation are: (i) saturation due to excited state interaction, (ii) true activator saturation, i.e. excitation of a

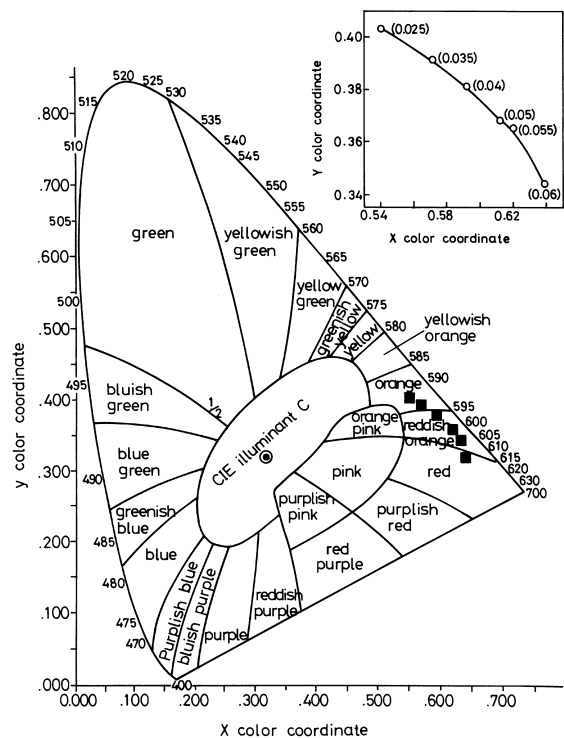


Fig. 7. CIE color loci of  $Y_2O_2S:Eu$  with various  $Eu/Y$  molar ratios. Inset is the exploded view of the  $x$ - and  $y$ -coordinates of specimens studied. The number in parentheses is the  $Eu/Y$  molar ratio.

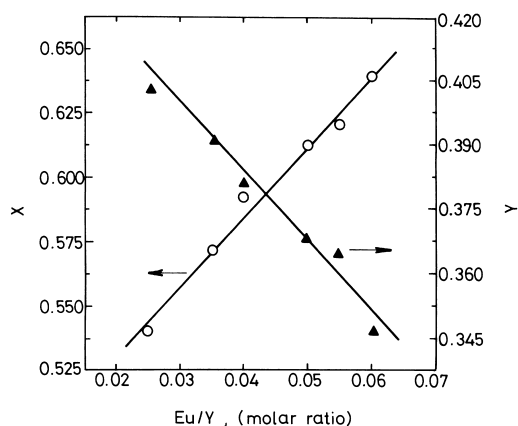


Fig. 8.  $x$ - and  $y$ -coordinate of CIE color coordinate of  $Y_2O_2S:Eu$  phosphor as a function of Eu concentration.

large fraction of available activator sites causing significant depletion of the ground state population, and (iii) saturation due to temperature rise [12].

If there are interactions between excited activators, additional energy loss mechanisms will arise, such as, one of the two excited activators in the interaction was forced to relax non-radiatively to the ground state, while the other is promoted to a higher excited state. Hence, The luminescence efficiency is decreased as manifested in the weak 530 and 583 nm peaks for samples with  $Eu/Y(0.025)$  as observed.

Fig. 6 gives a typical decay curve of the 626 nm luminescence ( ${}^5D_0 \rightarrow {}^7F_2$ ) under DYE laser excitation. The decay times are 1.1, 0.65, 0.5, 0.81, and 0.56 ms for samples with  $Eu/Y$  of 0.025, 0.035, 0.04, 0.055, and 0.06, respectively. The decay time is short enough and is suitable for CRT applications.

The CIE color coordinate is employed to analyze the luminescence color. The luminescence of  $Eu^{3+}$ -activated phosphors results from three excited states  ${}^5D_2$  (blue-green),  ${}^5D_1$  (green-orange), and  ${}^5D_0$  (red), as observed in the CL and PL spectra shown in Figs. 2 and 5.  $Y_2O_2S:Eu$  phosphor has the advantage of color shift. As observed from the CIE color loci shown in Fig. 7, the color of  $Y_2O_2S:Eu$  phosphor changes with Eu concentration, it shifts from orange (samples with  $Eu/Y = 0.025$  and  $0.035$ ) to red ( $Eu/Y = 0.06$ ) via reddish orange ( $Eu/Y = 0.045$  and  $0.055$ ). This also suggests that  $Y_2O_2S:Eu$  phosphor with  $Eu/Y = 0.06$  can be used as a red primary for color picture tubes.

The  $x$ - and  $y$ -coordinate of CIE color are proportional and inversely proportional to Eu concentration, respectively, as shown in Fig. 8. The reason for the linearity between the  $x$ - (and  $y$ -) coordinate and Eu content is not known yet.

However, this curve can be employed to fine tune the color by interpolating for appropriate Eu concentration.

#### 4. Conclusions

Europium-activated yttrium oxysulfide films have been prepared by electrophoretic deposition of flux grown  $Y_2O_2S:Eu$  powders on to ITO-coated glass substrates. Polycrystalline  $Y_2O_2S:Eu$  exhibits a hexagonal crystal structure with unit cell dimensions  $a = 0.37$  nm and  $c = 0.65$  nm. The CIE measurement reveals that the color of  $Y_2O_2S:Eu$  phosphor varies with the activator concentration. Increasing Eu concentration from 0.025 to 0.06, the phosphor color converts from orange to red. Both CL and PL spectra show the strongest emission line at 626 nm, suggesting a main electron transition level from  ${}^5D_0$  to  ${}^7F_2$ . The  ${}^5D_1/{}^5D_0$  intensity ratio decreases with the increase in Eu concentration, indicating that as more Eu is added, the luminescence color becomes redder but less bright.

#### Acknowledgements

This work is supported by the Electronics Research and Service Organization, Industrial Technology Research Institute (ERSO, ITRI), Hsinchu, Taiwan under contract no. E86014.

#### References

- [1] B.G. Yacobi, B.G. Holt, Cathodoluminescence Microscopy of Inorganic Solids, Plenum Press, New York, 1990.
- [2] A.G. Chakhovskoi, W.D. Kesling, J.T. Trujillo, C.E. Hunt, J. Vac. Sci. Technol. B12 (1994) 785.
- [3] L. Ozawa, Application of Cathodoluminescence to Display Devices, Kodansha Ltd., Tokyo, Japan, 1994, pp. 280–294.
- [4] M.P. Thi, A. Morell, J. Electrochem. Soc. 138 (1991) 1100.
- [5] O. Kanehisa, T. Kano, H. Yamamoto, J. Electrochem. Soc. 132 (1985) 2023.
- [6] Y. H. Tseng, Luminescence Phenomena of  $Y_2O_2S:Eu$  Red Phosphor, M.Sc. Thesis, National Chiao Tung University, Hsinchu, Taiwan, June 1997.
- [7] M.J. Shane, J.B. Talbot, B.G. Kinney, E. Slugky, K.R. Hesse, J. Colloid Interface Sci. 165 (1994) 334.
- [8] O.J. Sovers, T. Yoshioka J. Chem. Phys. 49 (1968) 4945.
- [9] W.D. Kingery, H.K. Bowen, D.R. Uhlmann, Introduction to Ceramics, 2nd Ed., Wiley, New York, 1976, p. 58.
- [10] A. Abdel-Kader, M.M. Elkholy, J. Mater. Sci. 27 (1992) 2887.
- [11] L. Ozawa, Application of Cathodoluminescence to Display Devices, Kodansha Ltd., Tokyo, Japan, 1994, pp. 28–29.
- [12] D.J. Robbins, J. Electrochem. Soc. 123 (1976) 1219.
- [13] L. Ozawa, Cathodoluminescence Theory and Applications, Kodansha Ltd., Tokyo, Japan, 1990, pp. 53–80.
- [14] S. Imanaga, S. Yokono, T. Hoshina, Jpn. J. Appl. Phys. 19 (1980) 41.